

Research on Wind Effects of Super Tall Buildings with Rounded Arcs, Triangles and Retracted Platforms

Mengran Xu¹, Chen Huang², Bingjun Dou¹

¹Zhejiang Infrastructure Construction Group Co., LTD., Hangzhou 310000, China

²China United Engineering Co., LTD., Hangzhou 31000, China

Keywords: Rounded Corner Arc-Edge Triangular, Setback, Wind-Load Characteristics, Wind Tunnel Tests, Wind-Induced Dynamic Response

Abstract: In order to explore the wind effect behaviors of rounded-corner arc-edge triangular super high-rise building with setbacks, a number of setback building models were designed. Through rigid-model simultaneous pressure measurement test, the influence of aerodynamic shape optimization schemes on the wind load and wind-induced response characteristics of the building was studied. The results indicate that the setbacks significantly reduced the overall along-wind shape coefficients of such buildings, and the wind pressure distribution on the building surface is considerably affected by the different forms of setback. The upper setback scheme can significantly reduce the base bending moment and shear force, but hardly affect the variation of base bending moment and shear force with the wind direction angle. The setbacks have little influence on the top-floor peak displacement, but can usually increase the top-floor peak cross-wind acceleration of the structure.

1. Overview

With the acceleration of urbanization, the deepening of economic construction and the shortage of land resources, the development of high-rise and super high-rise buildings is growing rapidly. In order to avoid the twisting effect of the structure caused by the irregular plane, high-rise buildings are usually designed for symmetrical cross sections such as rectangle, triangle and circle. Triangular buildings in order to avoid the formation of sharp corner space, more choose rounded corners and curved edges triangle plane.

In the field of wind engineering, the current research on high-rise buildings is more focused on rectangular section buildings [1-2], and the research on rounded angular triangle high-rise buildings is rare, but there are more and more engineering examples of such buildings. For example, super

high-rise buildings such as Guangzhou West Tower and Hangzhou New World Global Center all adopt this kind of cross section. Relevant researchers have also studied the wind load characteristics [3] of these buildings from the perspective of engineering application through wind tunnel tests. In other similar sections, Bandiet [4] studied the wind load characteristics of high-rise building models with equilateral triangle, shear angle equilateral triangle and clover shape under urban landform. However, these studies are based on specific engineering projects, and it is not clear whether the results and conclusions can be directly applied to similar buildings. In view of this, this paper designs several different types of deregistration models for super high-rise buildings with rounded corners and curved edges and triangular sections, and carries out simultaneous pressure measurement tests of rigid models to study the effects of different deregistration optimization schemes on the wind load and wind-induced response characteristics of buildings.

2. Overview of Wind Tunnel Pressure Measurement Test

2.1 Wind Tunnel Test Equipment and Wind Field

The wind tunnel test was conducted in the ZD-1 boundary layer wind tunnel of Zhejiang University. The schematic diagram of the wind tunnel is shown in Figure 1. Several measurement systems were used in this wind tunnel test. Dandy 4 channel hot wire anemometer system was used to debug and measure the simulated wind field of atmospheric boundary layer. The reference wind speed of the test flow field was measured and monitored by pitot tube and micromanometer. The multi-point simultaneous pressure measuring system was used to measure the wind pressure on the surface of the model. Based on Kwon et al's research on wind load specifications of many countries, the boundary layer wind field in this experiment simulates the Japanese Category IV landform under urban environment [5].

Compared with Category D in the GB standard [6] of China, the wind speed of Category IV landform in Japan is higher and the turbulence degree is lower. Therefore, the average force coefficient of Class IV landform is larger and the pulse dynamic coefficient is smaller than [7] that of class D landform.

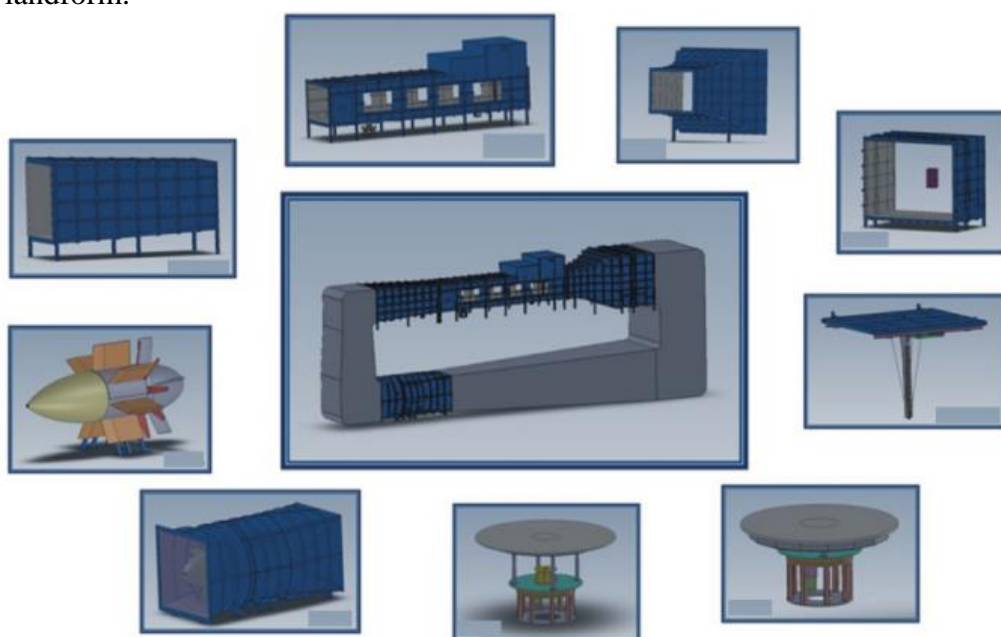


Figure 1. Schematic diagram of ZD-1 wind tunnel

2.2 Building Model and Pressure Test

The aerodynamic contour optimization test consists of four models: A round-corner curve-edge triangle cross section control model A with equal section, and three models B, C and D with different withdrawal schemes. All the models are retired twice, in which model C is obtained by rotating the middle section by 60 °on the basis of model B, and model D is obtained by rotating the upper two sections by 60 °on the basis of model B.

The scale ratio of the model is 1:300, the distance between the vertices of the rounded triangle on the bottom of the building prototype is 60m, the height is 300m (model height1000mm), and the height of the retreating part is 100m,200m. FIG. 2 shows the schematic diagram of the retreating model series.

The measuring point layer is arranged according to the principle of dense above and sparse below, and encrypted [8] within a certain range of the height of the retreating platform. Accordingly, a total of 11 measuring layers are set up along the height direction of the model. The size of the building prototype and the distribution of measuring point layers along the height are shown in Figure 3. The simultaneous pressure measurement test of rigid model is carried out for the series of models. With 5 °as one wind direction for each model, 72 wind direction tests from 0 °to 360 °were carried out, so as to obtain wind pressure data. The definition of wind direction of each model is shown in Figure 4.

3 The Influence of Backing on the Wind Load Characteristics of Buildings

3.1 Overall Body Type Coefficient

The downwind force of each test layer can be obtained by integrating the wind pressure of the test point of the building prototype according to its control area. F_s

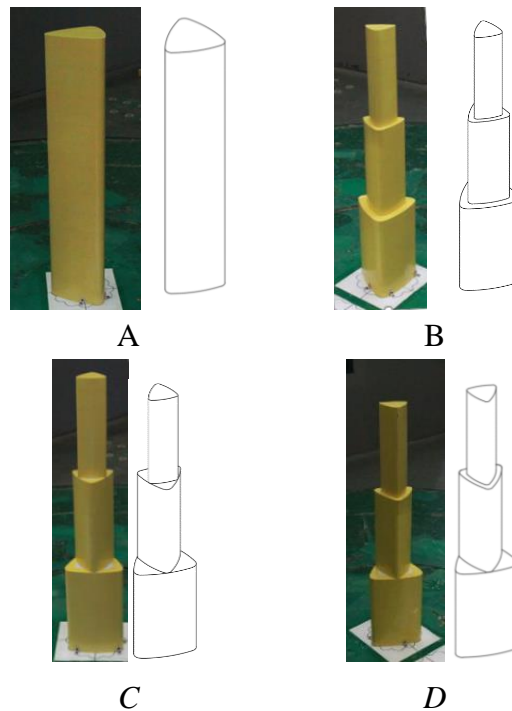


Figure 2. Schematic diagram of the 3D model

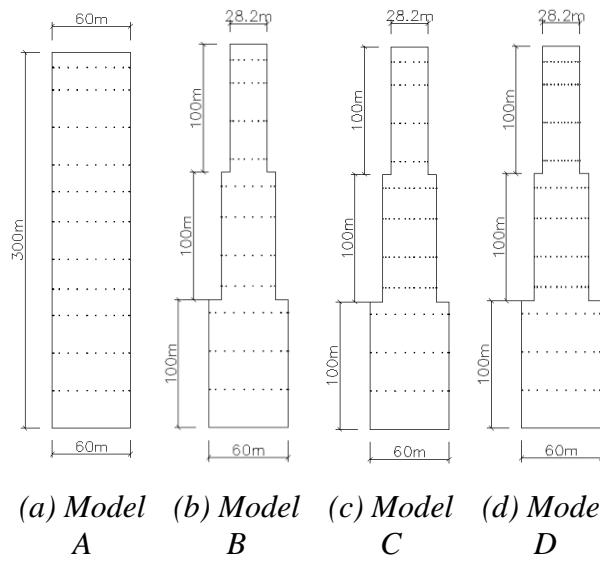


Figure 3. Model elevation and its measuring point layer arrangement

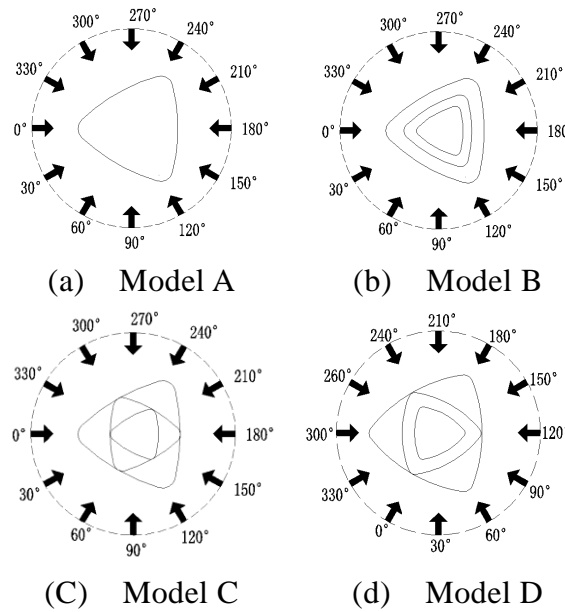


Figure 4. Definition of wind Angle for each model

The overall body shape coefficient of each measuring layer can be further obtained CS [9] by the following formula:

$$C_s(z_i) = \frac{F_s(z_i)}{w_0 \mu_{z_i} L_s} \quad (1)$$

Where: L_s represents the downwind control length of the measurement point layer; μ_{z_i} represents the wind pressure height change coefficient of the measuring point layer; w_0 represents the basic wind pressure.

FIG. 5 shows a comparison of the curve of the downwind overall body size coefficient envelope value with height for three different series models and standard model A. As can be

seen from the figure, the rollback and rollback rotation have a great influence on the downwind overall body size coefficient of the building, and there is an obvious abrupt change near the rollback and rollback rotation height, which decreases the coefficient values in the middle and lower part, while increases the coefficient values near the top, making the coefficient values of models C and D exceed the recommended values of the specification [10].

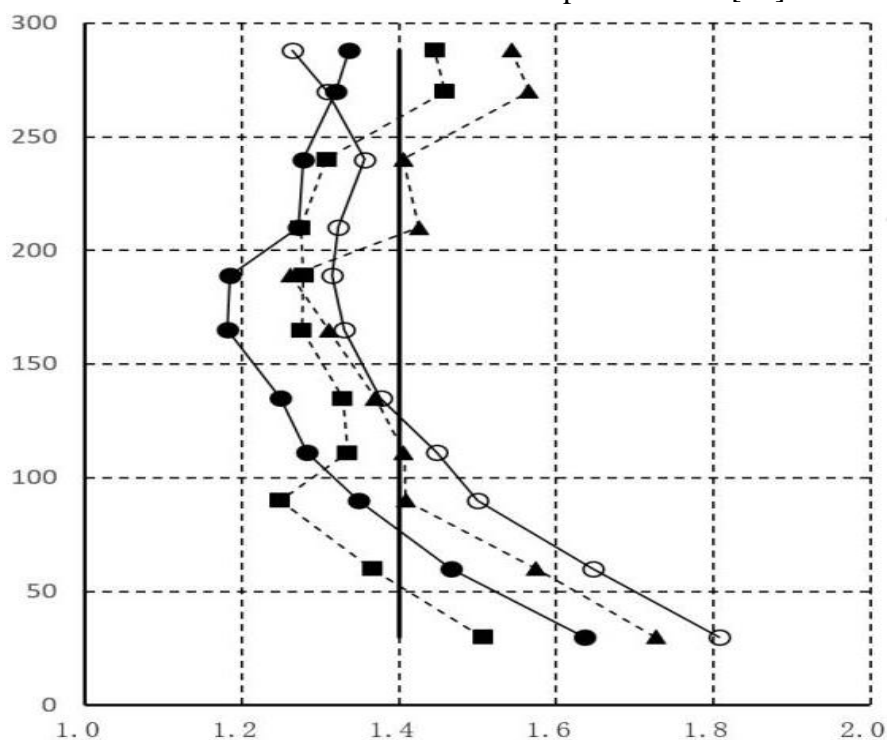


Figure. 5 Curve of the envelope value of the downwind overall body shape coefficient with height

3.2 Wind Pressure Distribution on Building Surface

The wind pressure distribution on the building surface is an important index to measure the aerodynamic performance of the building. Considering that the cross-section characteristics of rounded angular triangle vary significantly in wind direction, typical building surfaces under seven wind direction angles of 0° , 30° , 60° , 90° , 120° , 150° and 180° are selected as research objects, and their average wind pressure coefficient contour lines are drawn, as shown in Figure 6.

The results show that the wind direction Angle of the average wind pressure coefficient of the building surface presents an obvious change law. When a surface is on the leeward side, its wind pressure distribution is basically uniform, and the maximum value appears on the top of the building [11]. When the surface is on the windward side, most of the areas show positive pressure area, and the maximum value appears on the upper part of the building. When it is on the crosswind side, the wind pressure distribution regularity is poor, and it is greatly affected by different windward angles [12]. The detention has little effect on the average wind pressure distribution, while the detention rotation has a significant effect on the wind pressure distribution on the study surface, which makes the wind pressure change more violently at different positions along the direction of incoming flow.

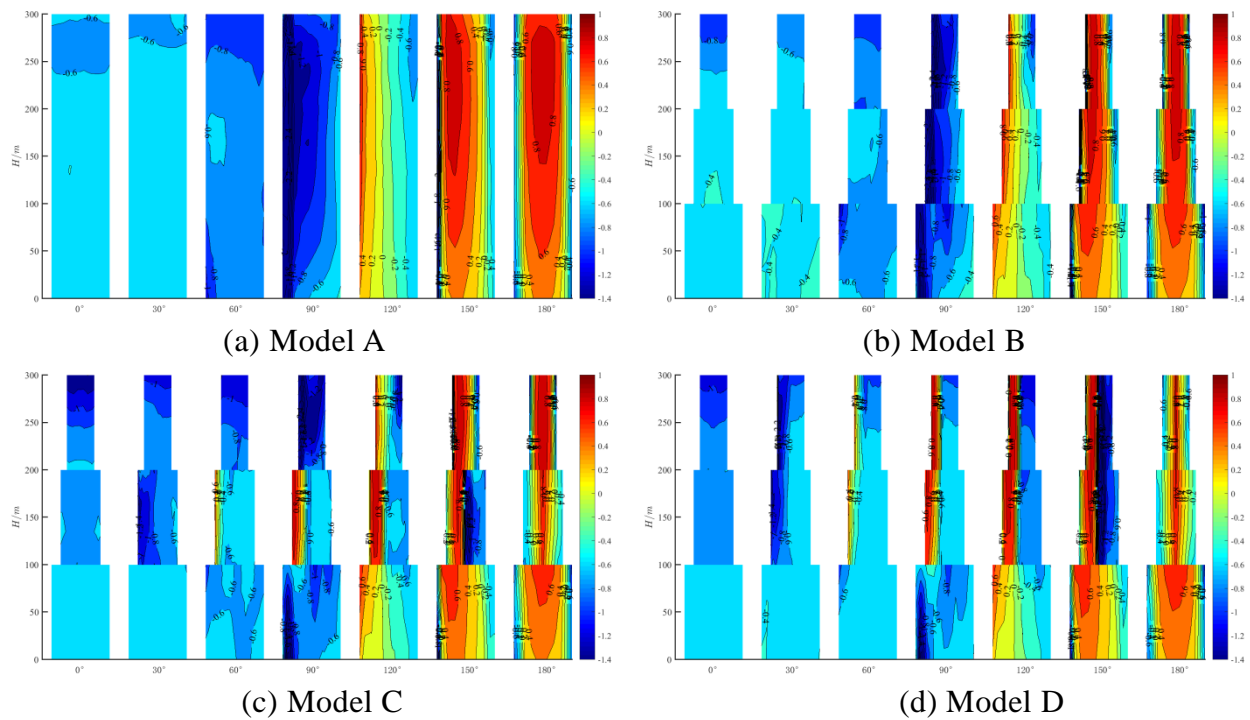


Figure 6. Average wind pressure distribution of building surface under different wind angles(kPa)

4 Influence of Backing on Wind Vibration Response of Building

According to the assumption of infinite stiffness in the floor plane, the mass and interlayer stiffness of each structural layer of the building are extracted, and then the equivalent simplified layer model of the structure is established according to the principle of finite element analysis. Newmark-P is used to calculate the dynamic response of the structure, and the peak displacement and peak acceleration of the structure layer under each working condition are obtained [13]. Through the calculation of dynamic characteristics, the first two natural vibration frequencies of the simplified layer model of each building are obtained, as shown in Table 1.

Table 1. shows the first two natural vibration frequencies of the model

The model	First stage	Second stage
A	0.133	0.136
B	0.180	0.183
C	0.180	0.183
D	0.180	0.183

4.1 Peak Acceleration at the Top of the Structure

Figure 7 ~ 10 shows the rose graph of the wind-wind variation of the peak acceleration of the four models in the downwind and crosswind direction. It can be seen that the peak accelerations of models B,C and D increase somewhat under the influence of the deplatform, but the peak accelerations of different models show similar periodic changes in the wind direction Angle. The period of the peak acceleration is 2/3 for both downwind and crosswind. The former reaches the maximum when the arc faces the wind, while the latter reaches the maximum when the asymmetric faces the wind[14].

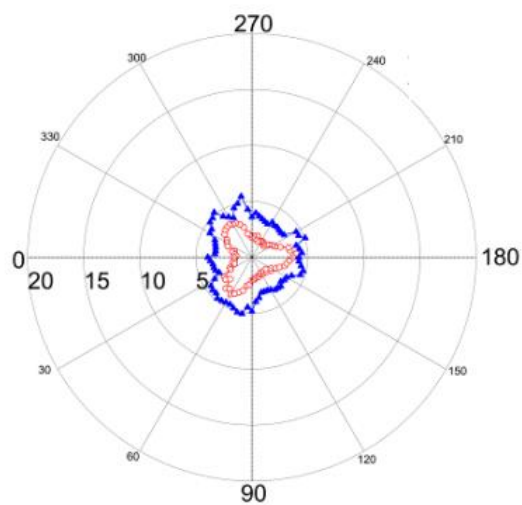


Figure 7. Rose diagram of peak acceleration of Model A

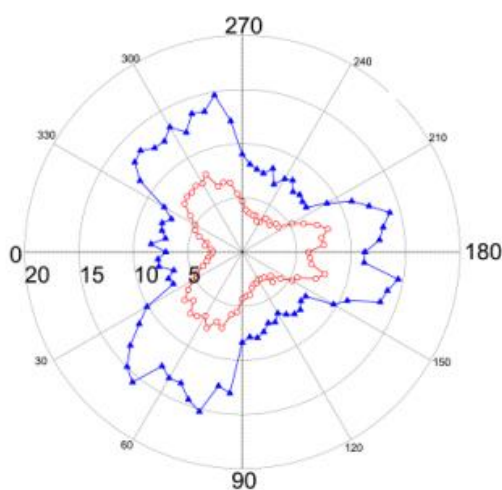


Figure 8. Rose graph of peak acceleration of model B

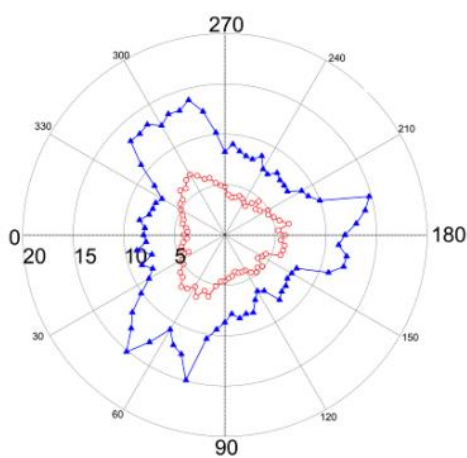


Figure 9. Rose diagram of peak acceleration for model C

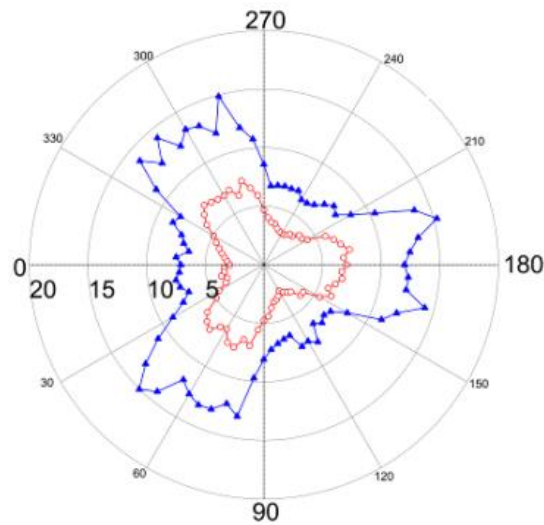


Figure 10. Rose diagram of peak acceleration for model D

4.2 Peak Displacement at the Top of Structure

Figure 11 ~ 14 shows the rose chart of the peak displacement at the top of the structure downwind and sideways for the four models. It can be seen from the figure that the top peak displacement changes in the same direction of different models are similar. The change period of the peak displacement at the top of the transverse wind direction is $1/3$, and the rose chart is hexagonal star, with the maximum value obtained when the asymmetric edge is facing the wind and the minimum value obtained when the arc edge is facing the wind[15]. The change period of the downwind peak displacement is $2/3$, and the maximum value is obtained when the arc edge is windward. Moreover, the displacement values of models C and D are relatively small due to the influence of different retreat rotation modes.

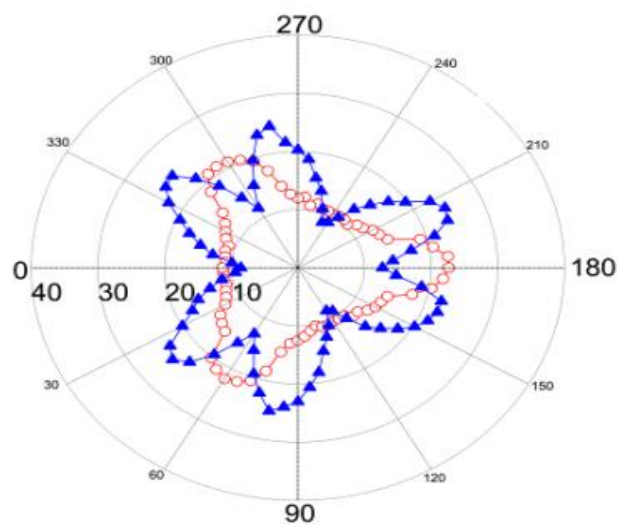


Figure 11. Rose diagram of peak displacement at the top of model A

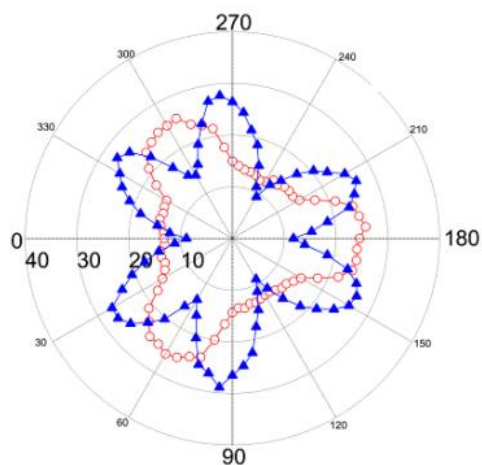


Figure 12. Rose diagram of peak displacement at the top of Model B

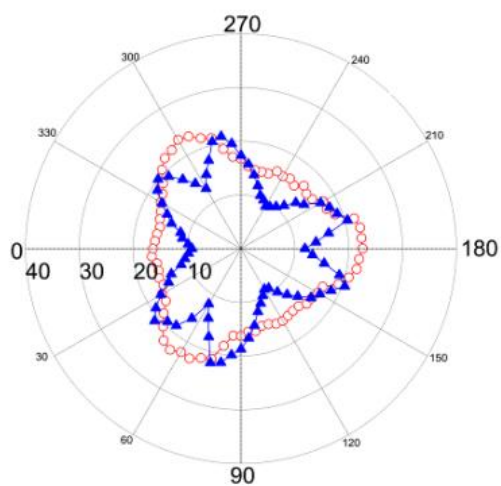


Figure 13. Rose diagram of peak displacement at the top of Model C

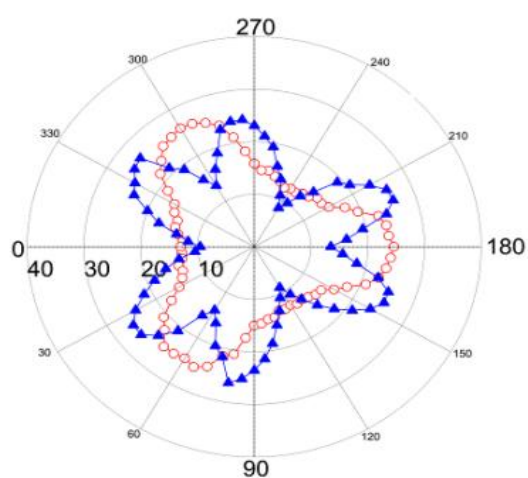


Figure 14. Rose diagram of peak displacement at the top of Model D

5 Conclusions

(1) The downwind overall body size coefficient of rounded angular triangle supertall buildings can be significantly reduced by back off; The value of the body shape coefficient can be further reduced by the back-off rotation.

(2) The two simultaneous detentions have little effect on the surface wind pressure distribution, while the detentions rotation has obvious effect on the surface wind pressure distribution, resulting in dramatic changes in different parts of the incoming flow direction.

(3) Different detentions schemes usually increase the peak acceleration of the top layer of the structure, but have little influence on the peak displacement of the top layer. The peak displacement of the detentions model C studied in this paper is even smaller than that of the equal-section model under the same landform.

(4) Detention can significantly reduce the equivalent wind load base bending moment and shear force of the building, but basically does not affect the change of the base bending moment and shear Angle in the wind.

Funding

If any, should be placed before the references section without numbering.

Data Availability

Data sharing is not applicable to this article as no new data were created or analysed in this study.

Conflict of Interest

The author states that this article has no conflict of interest.

References

- [1]Gu Ming, Ge Fu. *Wind disturbance characteristics of downwind layer of square tall buildings. Journal of Tongji University (Natural Science)*,2014,42(5): 665-671.
- [2]Gu Ming, Ge Fu, Han Ning. *Wind interference characteristics of transverse wind layer of square tall building. Journal of Tongji University (Natural Science)*,2014,42(8): 1147-1152.
- [3]Chen Qiang. *Study on wind load characteristics of rounded angular triangle tal buildings . J. Hangzhou: Zhejiang University, 2018.*
- [4]Bandi E K, Tamura Y, Yoshida A, et al. *Exper imental investigation on aerodynamic characteristics of various triangular-section high-rise buildings. Journal of Wind Engineering and Industrial Aerodynamics*,2013,12260-68.
- [5]Kwon D K, Kareem A. *Comparative study of major international wind codes and standards for wind effects on stall buildings. Engineering Structures*,2013,51:23-35.
- [6]*Load code for Building Structures: GB50009-2012*[SJ.Beijing:China Building and Construction Press,2012.
- [7]Ding Tong, Chen Shuifu. *Aerodynamic Characteristics of triangular super tall buildings with rounded corners and curved edges in different facade contraction forms. Journal of Vibration and Shock*, 2022,41(4);:70-76,133.
- [8]*Standard of wind tunnel test method for building engineering:JGJ/T 338-2014*[SJ. Beijing:China Architecture and Construction Press,2015.

- [9]Huang Bencai, Wang Congjun. *Principle and Application of Structural Wind Resistance Analysis*. 2nd Ed.Shanghai: Tongji University Press,2008.
- [10]Technical Specification for Concrete Structure of high-rise Building: JGJ3-2010.Beijing: China Building and Construction Press,2011.
- [11] Yu Xianfeng, Lin Yixin, Xie Zhuangning. *Research on Wind Load and Wind Effect of Super Tall Buildings under the Interference of Two Symmetric Buildings*. *Vibration and Impact*, 2021, 40 (21): 10-15,24.
- [12] Xu Haiwei, Chen Jiagan, Shen Guohui, Chen Shuifu. *Prediction of Wind Load Shape Coefficient for Rectangular Section Tall Buildings Based on Small Sample Machine Learning*. *Journal of Building Structures*, 2023,44 (11): 137-145.
- [13] Zou Lianghao, Pan Xiaowang, Fan Xingyan, Liang Shuguo. *Three dimensional equivalent static wind load of eccentric high-rise buildings based on equivalent internal force of each story*. *Journal of Hunan University (Natural Science Edition)*, 2023,50 (7): 109-119.
- [14] Li Yonggui, Quan Jia, Li Yi, Yan Jiahui, Hu Yang. *Research on the Influence of Turbulence Characteristics on Wind Load of Circular Tall Buildings*. *Journal of Natural Disasters*, 2023,32 (5): 149-156.
- [15] Xie Yishun, Xu Zidong, Wang Hao. *Wind induced comfort assessment of high-rise buildings based on large eddy simulation*. *Journal of Southeast University (English edition)*, 2023,39 (2): 127-132.